Jacqueline Stöckli,[1,2,3,4] Christopher C. Meoli,[1,2,3] Nolan J. Hoffman,[1,2,3] Daniel J. Fazakerley,[1,2,3] Himani Pant,[3] Mark E. Cleasby,[5] Xiuquan Ma,[3] Maximilian Kleinert,[3,6] Amanda E. Brandon,[3] Jamie A. Lopez,[3] Gregory J. Cooney,[3,4] and David E. James[1,2,3,7]

The RabGAP TBC1D1 Plays a Central Role in Exercise-Regulated Glucose Metabolism in Skeletal Muscle

Diabetes 2015;64:1914–1922 | DOI: 10.2337/db13-1489

Insulin and exercise stimulate glucose uptake into skeletal muscle via different pathways. Both stimuli converge on the translocation of the glucose transporter GLUT4 from intracellular vesicles to the cell surface. Two Rab guanosine triphosphatases-activating proteins (GAPs) have been implicated in this process: AS160 for insulin stimulation and its homolog, TBC1D1, are suggested to regulate exercise-mediated glucose uptake into muscle. TBC1D1 has also been implicated in obesity in humans and mice. We investigated the role of TBC1D1 in glucose metabolism by generating TBC1D1$^{-/-}$ mice and analyzing body weight, insulin action, and exercise. TBC1D1$^{-/-}$ mice showed normal glucose and insulin tolerance, with no difference in body weight compared with wild-type littermates. GLUT4 protein levels were reduced by ~40% in white TBC1D1$^{-/-}$ muscle, and TBC1D1$^{-/-}$ mice showed impaired exercise endurance together with impaired exercise-mediated 2-deoxyglucose uptake into white but not red muscles. These findings indicate that the RabGAP TBC1D1 plays a key role in regulating GLUT4 protein levels and in exercise-mediated glucose uptake in nonoxidative muscle fibers.

Insulin and exercise enhance muscle glucose uptake by triggering GLUT4 vesicles to translocate from within the cell to the plasma membrane (PM) (1,2). These stimuli activate different signaling pathways that converge on similar steps in the GLUT4 trafficking pathway. The identification of the Rab guanosine triphosphatase (GTPase)-activating protein (GAP) AS160/TBC1D4 as an Akt substrate was exciting because this provided a link between insulin signaling and GLUT4 trafficking (3). RabGAPs regulate the activity of Rab GTPases, which play an intimate role in eukaryotic vesicular trafficking (1,4). AS160 is localized to GLUT4 vesicles through its interaction with insulin-responsive aminopeptidase (IRAP), a constituent of GLUT4 vesicles (5–7). In the absence of insulin, AS160 is thought to be active, thus facilitating intracellular sequestration of GLUT4 by rendering the Rab associated with GLUT4 vesicles, possibly Rab10, inactive (8,9). Insulin stimulates Akt-dependent AS160 phosphorylation and 14-3-3 binding, leading to inactivation of AS160 GAP activity, increased GTP loading of Rab10, and increased GLUT4 translocation to the PM (1,10). Knockdown of AS160 in adipocytes increases PM GLUT4 levels, consistent with the role of AS160 as a negative regulator (5,11,12).

TBC1D1 is a close homolog of AS160 that is highly expressed in skeletal muscle and so has been postulated to play a role in exercise-mediated GLUT4 trafficking (13–17). AS160 and TBC1D1 have identical domain structures. They share 47% amino acid identity and display distinct tissue expression: AS160 is highly expressed in heart, white adipose tissue (WAT), and oxidative muscles, such as soleus, whereas TBC1D1 is expressed in muscle but is absent from WAT (14). The suggested mechanism

[1]Charles Perkins Centre, University of Sydney, Sydney, New South Wales, Australia
[2]School of Molecular Bioscience, University of Sydney, Sydney, New South Wales, Australia
[3]Garvan Institute of Medical Research, Sydney, New South Wales, Australia
[4]St Vincent's Clinical School, Faculty of Medicine, University of New South Wales, Sydney, New South Wales, Australia
[5]The Royal Veterinary College, University of London, London, U.K.
[6]Molecular Physiology Group, Department of Nutrition, Exercise and Sports, August Krogh Centre, University of Copenhagen, Copenhagen, Denmark
[7]School of Medicine, University of Sydney, Sydney, New South Wales, Australia

Corresponding author: David E. James, david.james@sydney.edu.au.

Received 28 September 2013 and accepted 24 December 2014.

J.A.L. is currently affiliated with the Peter MacCallum Cancer Centre, Department of Oncology, University of Melbourne, Parkville, Victoria, Australia.

for TBC1D1 regulation is primarily based on the well-known regulation of its close homolog AS160. TBC1D1 interacts with IRAP (18), inactivates the same Rabs as AS160 (13), and binds 14-3-3 upon phosphorylation (16,19). Although Akt mediates AS160 phosphorylation on the crucial 14-3-3 binding sites, linking AS160 to insulin signaling, TBC1D1 binds 14-3-3 in response to AMPK activation, a kinase activated by exercise (2).

A mutation in TBC1D1 (R125W) is linked to human obesity (20,21), although the precise role of this mutation in TBC1D1 function is not known. Several mouse models with reduced TBC1D1 expression have been described, including a congenic model that contains a locus from the Swiss Jim Lambert strain, and a gene trap knockout (22–25). These mice show no change in body weight or reduced body weight; reduced glucose uptake into isolated white muscle in response to various agonists, including insulin, contraction, or AICAR, an AMPK agonist; and increased fatty acid oxidation at the whole-body level and in muscle. In general, no defect in whole-body insulin-mediated glucose metabolism was found (22–25).

We generated a TBC1D1$^{-/-}$ mouse model back-crossed onto the C57Bl6 background for >10 generations. These mice had no defect in whole-body insulin-mediated glucose metabolism, unchanged body weight, and no difference in high-fat diet (HFD)–induced obesity or insulin resistance compared with wild-type (WT) littermates. They did, however, show impaired exercise endurance, which was likely caused by impaired AMPK agonist–mediated glucose uptake into muscle in vitro and impaired exercise-mediated glucose uptake in vivo, highlighting the important role of TBC1D1 in exercise-regulated glucose metabolism in muscle.

RESEARCH DESIGN AND METHODS

Materials

General chemicals were from Sigma-Aldrich Chemical Company, unless otherwise stated. Antibodies were from Sigma-Aldrich (Flag), Cell Signaling Technology (TBC1D1, AMPK, pT172 AMPK), Santa Cruz Biotechnology (14-3-3), Mito Sciences (mito-profile), Symansis (p642-AS160), and Molecular Probes (cyclooxygenase, complex IV). Antibodies against AS160 (5), GLUT4 (26), and GLUT1 (27) have been previously described. BSA was obtained from Bovogen Biologicals, and protease inhibitors were from Roche.

Generation of TBC1D1$^{-/-}$ mice

TBC1D1$^{-/-}$ mice were generated using a TBC1D1 gene-trap ES cell line from BayGenomics (#RRR502). The gene-trap vector insertion resulted in a truncated TBC1D1 mRNA. Heterozygous mice were generated by the Australian Phenomics Network ES to Mouse service at Monash University. Mice were genotyped by PCR and real-time PCR using the following primers within the gene-trap vector: 5′-gcggcaccgcgcctttcggcgg-3′ and 5′-ggaagggctggtcttcatccac-3′. Mice were backcrossed onto C57Bl/6 background and heterozygous ($^{+}/_{-}$) TBC1D1 breeding pairs produced TBC1D1$^{-/-}$ and WT littermates for experiments. Mice were group housed on a 12-h light/dark cycle with free access to food and water. Mice were fed ad libitum a standard laboratory chow (8% of calories from fat) or a HFD (Hugo's Copha, 48% fat [7:1 lard-to-safflower oil ratio], 32% carbohydrate, 20% protein). All experimental procedures were approved by the Garvan Institute/St Vincent's Hospital Animal Ethics Committee and followed the guidelines issued by the National Health and Medical Research Council Australia.

Glucose and Insulin Tolerance Tests and Insulin Measurements

Male littermates (12–16 weeks old) were fed standard chow or the HFD for 4 weeks. Mice were fasted for 6 h or overnight before glucose or insulin tolerance tests, respectively. Glucose (1 g/kg) or insulin (1 unit/kg) was administered by intraperitoneal injection, blood samples were obtained from the tail, and glucose was measured using an Accu-Chek Performa glucometer (Roche Diagnostics). Insulin was measured from whole blood using an insulin ELISA kit (Crystal Chem).

In Vivo Electroporation

In vivo electroporation of DNA into mouse tibialis anterior (TA) muscle was done under anesthesia, as previously described (28). Briefly, DNA was injected into the TA muscle. Immediately after the injection, 8 pulses of 200 V/cm and 20 ms at 1 Hz were administered across the distal limb via tweezer electrodes attached to an ECM-830 electroporator (BTX).

Exercise Experiments

Exercise experiments were performed on an Exer3/6 mouse treadmill (Columbus Instruments) at a 5% incline. Mice (15–21 weeks) underwent a 2-day period of treadmill running acclimatization that consisted of running for 15 min at a speed of 10 m/min on day 1 and for 15 min at 10 m/min, followed by 15 min at 13 m/min on day 2. Exercise was performed as indicated until exhaustion, defined as falling off the treadmill three times within 15 s.

In Vitro Glucose Uptake Into Isolated Muscle

[^{3}H]-2-deoxyglucose ([^{3}H]-2DOG) uptake into isolated extensor digitorum longus (EDL) and soleus muscles was performed as previously described (29). Muscles were incubated in the absence or presence of 100 nmol/L insulin (Calbiochem) or 2 mmol/L 5-aminoimidazole-4-carboxamide ribonucleotide (AICAR; Toronto Research Chemicals) for 20 min at 30°C.

Surgical Procedures and In Vivo Exercise-Mediated Glucose Uptake

Mice were anesthetized with isoflurane anesthesia for insertion of a polyurethane catheter into the left carotid artery. The free catheter end was tunneled under the skin, externalized at the neck, and sealed. Mice were then singly housed and monitored daily. Catheters were flushed every 1–2 days with heparinized saline to maintain patency. At 5–8 days after surgery, mice were fitted with an extension catheter and run on a treadmill with

speed gradually increasing to 16.5 m/min. [^{3}H]-2DOG (0.2 mCi/kg) was administered via the catheter, and blood samples were taken throughout the experiment. After 20 min, mice were killed and tissues removed and snap frozen. Exercise-mediated glucose uptake into red and white quadriceps was measured using AG 1-X8 Resin (BioRad) to remove glucose 6-phosphate and measuring tracer in the starting material (total [^{3}H]-2DOG) and the flow-through (nonphosphorylated [^{3}H]-2DOG) of the AG 1-X8 column, as previously described (30).

Quantitative Real-Time RT-PCR Assays

RNA extraction was performed using TRIZOL reagent (Life Technologies, Carlsbad, CA), following the manufacturer's protocol. Omniscript RT Kit (Qiagen) was used for cDNA synthesis. Real-time RT-PCR analysis was performed on Light Cycler 480 (Roche Applied Science) with Universal Probe Master System. Primers and probes for *GLUT4* mouse gene were selected according to the Universal Probe Library System (Roche Applied Science). The *Cyclophilin* gene was used as a control. The primers 5′-gacggacactccatctgttg-3′ and 5′-gccacgatggagacatagc-3′ were used for *GLUT4,* and 5′-ttcttcataaccacagtcaagacc-3′ and 5′-accttccgtaccacatccat-3′ were used for *Cyclophilin*.

Glycogen Measurements

Glycogen was measured as described (31). Briefly, tissues were dissolved in 1 mol/L KOH, and glycogen was precipitated twice with 95% ethanol. The glycogen pellet was resuspended in amyloglucosidase solution (0.3 mg/mL amyloglucosidase in 0.25 mol/L acetate buffer [pH 4.75]) and incubated overnight at 37°C. Glucose was determined using a calorimetric glucose oxidase kit (ThermoFisher Scientific).

Triglyceride, Nonesterified Fatty Acids, and Lactate Measurements

Calorimetric assays were performed according to the manufacturer's instructions to measure triglycerides (Roche) and nonesterified fatty acids (NEFAs; Wako) in plasma from mice. For lactate measurements, plasma was deproteinized, and lactate was measured as previously described (32,33).

Tissue Lysates, SDS-PAGE, and Immunoblotting

Mice were killed by cervical dislocation for tissue isolation. Tissues were lysed (20 mmol/L HEPES [pH 7.4], 250 mmol/L sucrose, 1 mmol/L EDTA, 2% SDS, protease inhibitors). Immunoblotting was carried out as previously described (5). Quantification of immunoblots was performed using Odyssey IR imaging system software.

Statistical Analysis

Data are expressed as mean and SEM unless indicated otherwise. *P* values were calculated by *t* test, one-way ANOVA, or two-way ANOVA using GraphPad Prism software.

RESULTS

GLUT4 Protein Levels Are Reduced in Muscle From TBC1D1$^{-/-}$ mice

TBC1D1$^{-/-}$ mice were generated using a gene-trap ES cell line (Fig. 1). There was no detectable TBC1D1 protein in muscles from TBC1D1$^{-/-}$ mice (Fig. 2*A*). The insertion of the gene trap resulted in a putative truncated TBC1D1 construct, fused to β-galactosidase and neomycin transferase. However, this putative TBC1D1 truncation was not detectable. AS160 protein levels were highest in heart, soleus, WAT, and red quadriceps and very low in white quadriceps, TA, and EDL. AS160 levels were not changed in tissues from TBC1D1$^{-/-}$ mice compared with WT littermates (Fig. 2*A* and *B*). GLUT4 levels were significantly reduced in muscle from TBC1D1$^{-/-}$ mice, with the most pronounced decrease in muscles with low endogenous AS160 expression. GLUT4 protein levels were significantly reduced in white quadriceps, TA, and EDL by 45%, 42%, and 37%, respectively (Fig. 2*A* and *B*). No significant change occurred in GLUT4 mRNA in TA muscle between the genotypes, indicating that reduced GLUT4 in TBC1D1$^{-/-}$ muscle occurs posttranscriptionally (Fig. 2*C*), consistent with recent findings (22–24). There was no compensatory upregulation in the level of GLUT1 (Fig. 2*B*).

TBC1D1 Overexpression Increases GLUT4 Protein Levels

To determine if TBC1D1 expression can rescue GLUT4 levels, Flag-TBC1D1 cDNA was injected into the right leg of mice, followed by in vivo electroporation. The left leg was injected with empty vector. One week later, TA

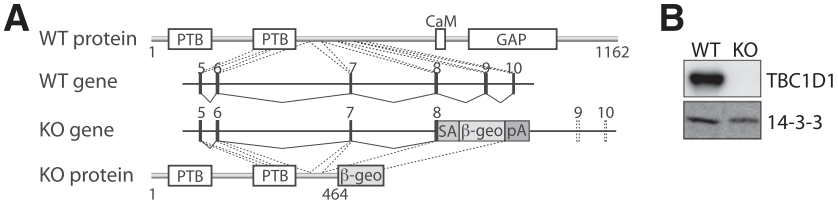

Figure 1— TBC1D1$^{-/-}$ mice genotyping. *A*: Diagram depicts endogenous protein and genomic DNA of WT and TBC1D1$^{-/-}$ (KO) location in RRR502 ES cell line with predicted truncated TBC1D1 protein. β-geo, fusion of β-galactosidase and neomycin transferase; CaM, calmodulin binding domain; pA, SV40 polyadenylation signal; PTB, phosphotyrosine binding domain; SA, splice acceptor site. *B*: TBC1D1 protein and 14-3-3 loading control in TA muscle from WT and TBC1D1 KO mice.

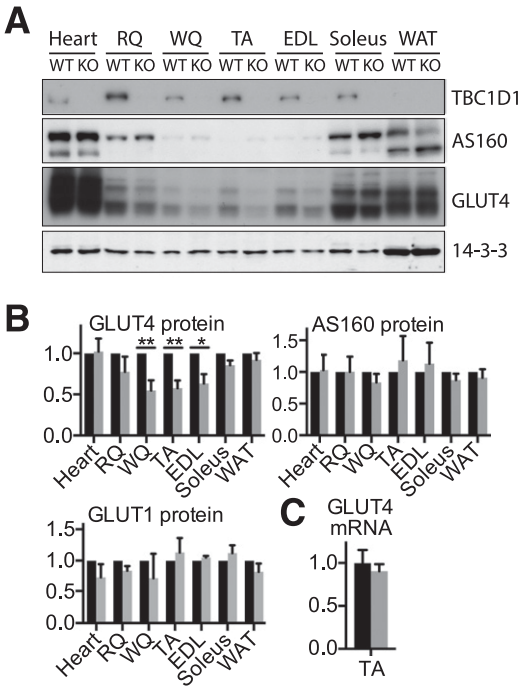

Figure 2—GLUT4 protein levels are reduced in TBC1D1$^{-/-}$ muscle. Tissues from WT and TBC1D1$^{-/-}$ (KO) littermates were isolated and immunoblotted with indicated antibodies. *A*: Representative immunoblots are shown. *B*: Immunoblots were quantified and normalized to WT protein levels. WT is shown in black bars and KO in gray bars (n = 3–4). *C*: GLUT4 mRNA levels in TA of WT and TBC1D1 KO mice, normalized to WT (n = 3). RQ, red quadriceps; WQ, white quadriceps. Error bars show the SEM. *P < 0.05, **P < 0.01.

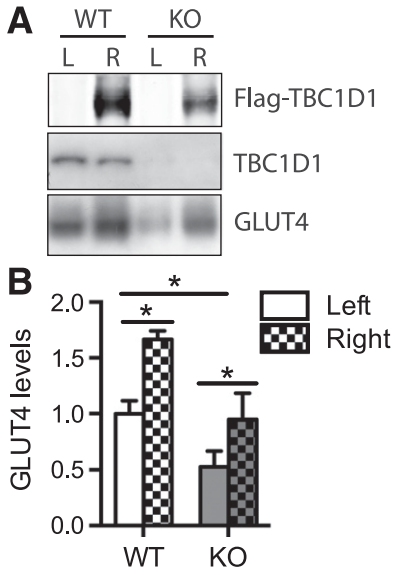

Figure 3—TBC1D1 overexpression increases GLUT4 levels. *A*: In vivo electroporation of endotoxin-free Flag-TBC1D1 (human) DNA into right leg (R) and endotoxin-free empty vector DNA into left leg (L) of WT and TBC1D1$^{-/-}$ (KO) mice. Mice were killed after 1 week, tissues were isolated, and TA muscles were immunoblotted with antibodies against Flag, TBC1D1, and GLUT4. Representative immunoblots are shown. *B*: Quantification of data in *A* (n = 3). The error bars show the SEM. *P < 0.05.

muscle lysates from left and right legs were immunoblotted with antibodies against Flag, TBC1D1, and GLUT4. Flag-tagged TBC1D1 was only detected in the TA muscle from the right leg (Fig. 3*A*). The TBC1D1 antibody selectively recognizes mouse but not human TBC1D1 and therefore does not recognize the overexpressed TBC1D1. GLUT4 levels were increased in TA that expressed Flag-TBC1D1 compared with the control leg in WT and TBC1D1$^{-/-}$ mice by 67% and 79%, respectively (Fig. 3*A* and *B*).

TBC1D1$^{-/-}$ Mice Have Normal Insulin-Mediated Glucose Metabolism and Body Weight

No difference was observed in glucose or insulin tolerance between TBC1D1$^{-/-}$ and WT littermates (Fig. 4*A* and *J*). In the insulin tolerance test for both genotypes, the glucose levels increased initially before dropping, as previously reported (34), likely due to a stress response (Fig. 4*J*). There was no difference in body weight in mice fed the chow or HFD, epididymal fat pad weight, fasting insulin levels, insulin levels during glucose tolerance tests, or glucose tolerance in response to the HFD between TBC1D1$^{-/-}$ and WT mice (Fig. 4).

TBC1D1$^{-/-}$ Mice Show Impaired Exercise Endurance

We next examined the exercise performance of TBC1D1$^{-/-}$ mice compared with WT littermates. Mice were subjected to exercise running on a treadmill, and two different exercise protocols were used to determine exercise endurance as determined by the total running time during low-intensity exercise, and maximal exercise capacity, determined by maximal running speed during high-intensity exercise. TBC1D1$^{-/-}$ mice showed a significant impairment in exercise endurance compared with WT littermates (Fig. 5*A* and *B*), but not in maximal exercise capacity (Fig. 5*C*).

There was no difference in muscle wet weight, mitochondrial oxidative phosphorylation protein levels, muscle glycogen levels at rest or after exercise, plasma levels of NEFA, and lactate between the genotypes (Fig. 6). There was a significant difference in plasma TGs between TBC1D1$^{-/-}$ and WT mice after exercise (Fig. 6*C*).

AMPK Agonist-Mediated Glucose Uptake Into Muscle Is Impaired in TBC1D1$^{-/-}$ Mice

We next sought to examine whether the absence of TBC1D1 affected insulin- or AMPK-induced glucose uptake. EDL and soleus muscles were isolated from TBC1D1$^{-/-}$ and WT littermates, mounted on muscle holders, and incubated in vitro. Muscles were incubated in the absence or presence of insulin or the AMPK agonist AICAR, and glucose uptake was measured using [^{3}H]-2DOG tracer accumulation (Fig. 7). [^{3}H]-2DOG uptake was significantly reduced in EDL from TBC1D1$^{-/-}$ mice, but this was not the case for soleus (Fig. 7*A*). This is likely due to decreased GLUT4 levels in EDL from TBC1D1$^{-/-}$ mice because insulin-stimulated AS160 phosphorylation was

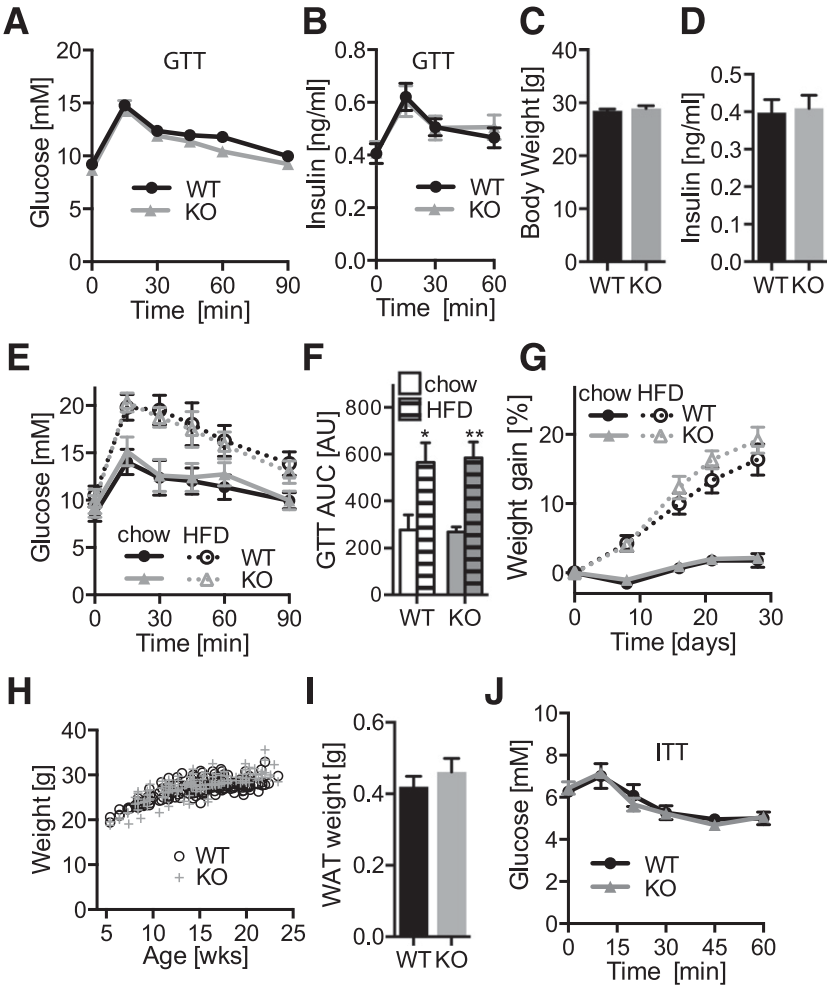

Figure 4—Chow- and HFD-fed TBC1D1$^{-/-}$ (KO) mice have glucose/insulin tolerance and body weights similar to those of their WT littermates. WT and TBC1D1 KO mice (12–16 weeks) were studied at baseline (*A–D*) and after 4 weeks of the chow or HFD (*E–G*). *A*: Baseline glucose tolerance test (GTT; n = 15–18). *B*: Insulin during glucose tolerance test (n = 9–10). *C*: Baseline body weight (n = 15–18). *D*: Fasted (6-h fast) insulin (n = 11). *E*: Glucose tolerance test after 4 weeks of the chow or HFD (n = 5–7). *F*: Area under the curve (AUC) of glucose tolerance test data in *E*. *G*: Weight gain on chow or HFD (%) (n = 6–9). *H*: Body weight of 6- to 23-week-old WT and KO mice (n = 25–30). *I*: Epididymal WAT weight (n = 8). *J*: Insulin tolerance test (ITT) (n = 6–7). Error bars show the SEM. *P < 0.05, **P < 0.01 vs. chow.

normal in these muscles (Fig. 7*C*). When [^{3}H]-2DOG uptake was analyzed as fold over basal, insulin significantly stimulated [^{3}H]-2DOG uptake in EDL from WT and TBC1D1$^{-/-}$ mice by 1.9- and 1.8-fold, respectively (Fig. 7*B*). In soleus muscle, insulin resulted in a 2.9-fold increase in [^{3}H]-2DOG uptake in WT and a 2.5-fold increase in TBC1D1$^{-/-}$ mice. AICAR significantly stimulated [^{3}H]-2DOG uptake by 1.6-fold in WT EDL and by 1.4-fold in WT soleus. In contrast, AICAR-stimulated [^{3}H]-2DOG uptake was significantly impaired in TBC1D1$^{-/-}$ muscles compared with WT muscles, with no significant increase over basal [^{3}H]-2DOG uptake. This was not due to defective AMPK activation because AICAR increased AMPK phosphorylation in EDL to a similar extent in WT and TBC1D1$^{-/-}$ mice (Fig. 7*C*). These data indicate that TBC1D1 plays a specific role in AICAR-mediated but not in insulin-dependent glucose uptake into white muscle.

Exercise-Mediated Glucose Uptake Is Reduced in White Muscle of TBC1D1$^{-/-}$ Mice

The impairment in [^{3}H]-2DOG uptake in response to AICAR in TBC1D1$^{-/-}$ muscles indicates that impaired glucose uptake might be the reason for the reduction in exercise endurance observed in these mice. We next determined [^{3}H]-2DOG uptake into muscle during exercise in WT and TBC1D1$^{-/-}$ mice. Because TBC1D1$^{-/-}$ and WT mice had the same maximal exercise capacity (Fig. 5), they were both exercised at the same speed of 16.5 m/min to achieve the same relative exercise intensity. Mice from both genotypes were able to complete the task. Exercise significantly increased [^{3}H]-2DOG uptake into WT red quadriceps by 15-fold and in white quadriceps by 8-fold (Fig. 8). Notably, [^{3}H]-2DOG uptake into white quadriceps was 6–8 times less than into red quadriceps (Fig. 8*A*). Although [^{3}H]-2DOG uptake into red quadriceps in TBC1D1$^{-/-}$

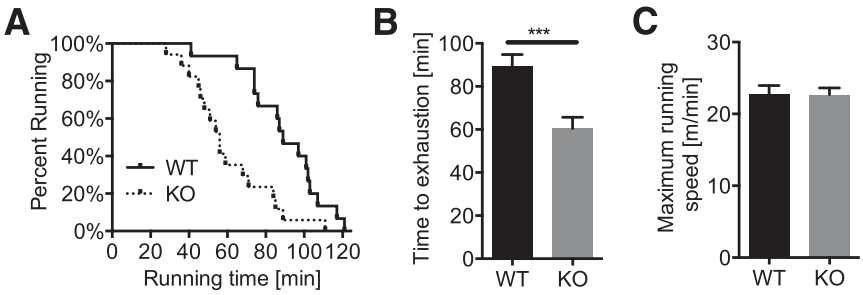

Figure 5—TBC1D1$^{-/-}$ mice have impaired exercise endurance. *A*: Survival plot showing the percentage of WT and TBC1D1$^{-/-}$ (KO) littermates running at indicated times during an exercise endurance test (10 min at 10 m/min with an increase in running speed by 1 m/min every 15 min). Total running time was determined until exhaustion. Individual data points are shown. *B*: Average and SEM of data shown in *A* (n = 15–17). *C*: Maximal running speed of WT and TBC1D1 KO littermates was determined during a maximal exercise capacity test (start at 8 m/min with an increase in running speed by 2 m/min every 1.5 min). Maximal running speed at exhaustion was determined (n = 15–17). The error bars show the SEM. ***P < 0.001.

mice was similar to that observed in WT mice, [^{3}H]-2DOG uptake into white quadriceps from TBC1D1$^{-/-}$ mice was reduced by 54% (Fig. 8*B*).

DISCUSSION

Members of the RabGAP family have generated much interest in the context of glucose metabolism. AS160 plays an important role in insulin-stimulated glucose uptake in fat and muscle cells (1,35), and mutations in AS160 are associated with severe insulin resistance in humans (36,37). The AS160 homolog TBC1D1 is involved in contraction-mediated glucose uptake (24) and has been implicated in obesity (20,21). In the current study, we show that TBC1D1$^{-/-}$ mice have no disruption in whole-body insulin action but impaired exercise-regulated metabolism. This is based on the following: *1*) AICAR-mediated [^{3}H]-2DOG uptake into isolated muscle was impaired in TBC1D1$^{-/-}$ mice (Fig. 7), *2*) exercise-mediated [^{3}H]-2DOG uptake into white quadriceps was significantly reduced in TBC1D1$^{-/-}$ mice in vivo (Fig. 8), and *3*) TBC1D1$^{-/-}$ mice exhibited reduced exercise endurance (Fig. 5).

The impairment in exercise endurance in TBC1D1$^{-/-}$ mice (Fig. 5) clearly implicates TBC1D1 as having an important role in exercise-regulated glucose metabolism. This defect could not be attributed to changes in muscle weight, the levels of mitochondrial oxidative phosphorylation proteins, or plasma lactate or NEFA levels, or muscle glycogen levels (Fig. 6), so it is likely due to the impairment in the ability of the exercising white muscle to import extracellular glucose (Fig. 8). White and red muscle fibers are both engaged during the treadmill exercise used for this test because we observed a decline in glycogen levels in both muscle types after a single bout of exercise (Fig. 6), consistent with previous studies (38). Although glucose uptake into white muscle was considerably less than into red muscle (Fig. 8*A*), it is plausible that the loss of TBC1D1 results in an impairment of glucose uptake into specific fibers that ultimately fatigue faster and lead to an overall exercise impairment. These data suggest that white muscle fibers likely play a crucial role even in endurance-style exercise and that a defect in these fibers may be a limiting factor in long-term endurance. However, whether the defect in exercise-mediated glucose uptake can be directly attributed to loss of TBC1D1 or the parallel decrease in GLUT4 protein levels is unclear. The greater defect we observed in AICAR compared with insulin-dependent glucose uptake in EDL (Fig. 7) is consistent with the defect being primarily due to loss of TBC1D1. Given that TBC1D1 is a major AMPK substrate in muscle (16,19,39), this would support the view that AMPK is a major determinant of exercise-regulated glucose metabolism in muscle. Although the role of AMPK in exercise-mediated glucose uptake has been controversial (40,41), a recent study demonstrated that muscle-specific AMPK β1/β2$^{-/-}$ mice also display impaired exercise endurance (42).

Our data, combined with results of other studies, are consistent with intramuscular energy stores, such as phosphocreatine and glycogen, in providing the energy needed during the initial phase of exercise, followed by a gradually increasing reliance on extracellular glucose when exercise is sustained. An impairment in this process would appear to have a major effect on endurance, giving rise to the concept that increased expression of TBC1D1 and/or AMPK might lead to improved endurance is worthy of future study. One difference we observed between WT and TBC1D1$^{-/-}$ mice after exercise, in addition to impaired exercise-mediated glucose uptake, was a significant reduction in plasma TG levels (Fig. 6). That fatty acid oxidation is increased in the TBC1D1$^{-/-}$ mice during exercise is possible, consistent with reports about a switch in fuel usage in other TBC1D1$^{-/-}$ mouse models (22,23). However, this is unlikely to be the cause of impaired endurance but rather a consequence of reduced glucose uptake.

The lack of any detectable body weight phenotype in TBC1D1$^{-/-}$ mice fed the chow or HFD (Fig. 4) was curious in light of previous studies (22–25). Initial studies used a congenic strain containing a Swiss Jim Lambert

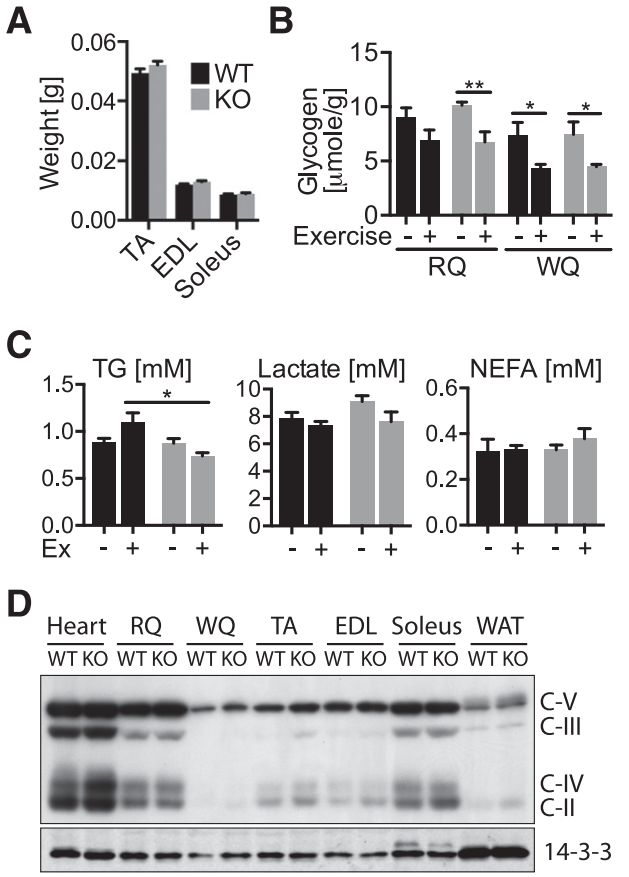

Figure 6—No difference in muscle tissue weights, mitochondrial oxidative phosphorylation protein levels, or glycogen. *A*: TA, EDL, and soleus were isolated and weighed from WT and TBC1D1$^{-/-}$ (KO) mice (n = 8). *B*: Muscle glycogen was measured in red quadriceps (RQ) and white quadriceps (WQ) from WT and TBC1D1 KO littermates after resting or exercise (Ex) (treadmill running for 55 min: 10 min at 10 m/min with an increase in running speed by 1 m/min every 15 min; n = 11–15). WT is shown in black bars and KO in gray bars. *C*: TGs, lactate, and NEFAs were measured in plasma from WT and TBC1D1 littermates after resting or exercise (see in *B*) (n = 5–8). *D*: Indicated tissues were immunoblotted for mitochondrial oxidative phosphorylation proteins using a mito-profile cocktail that includes antibodies against subunits of complex II (C-II), complex III (C-III), complex IV (C-IV), and complex V (C-V). Antibody against 14-3-3 was used as a loading control (n = 3). Error bars show the SEM. hr, hours. *P < 0.05, **P < 0.01.

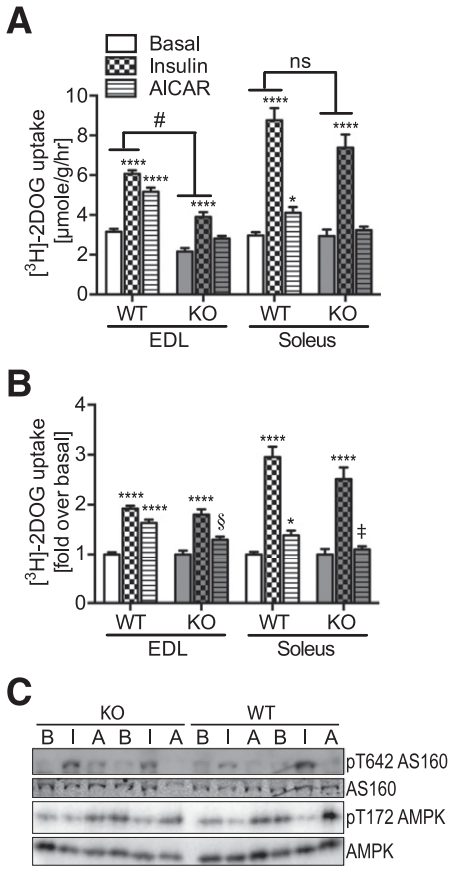

Figure 7—AICAR-stimulated glucose uptake is impaired in TBC1D1$^{-/-}$ muscle. Isolated EDL or soleus muscle from WT or TBC1D1$^{-/-}$ (KO) littermates was incubated in the presence or absence (B) of 100 nmol/L insulin (I) or 2 mmol/L AICAR (A), and [^{3}H]-2DOG uptake was measured (n = 9–25). *A*: [^{3}H]-2DOG uptake is shown. *B*: [^{3}H]-2DOG uptake data in *A* are presented as fold over basal. *C*: EDL muscles were immunoblotted with indicated antibodies. Error bars show the SEM. ns, not significant. *P < 0.05 vs. basal, ****P < 0.0001 vs. basal. #P < 0.0001 vs. WT. §P < 0.01 vs. WT. ‡P < 0.05 vs. WT.

locus with a mutation in the TBC1D1 gene that resulted in reduced body weight on the HFD but not on chow (24,25). A more recent study with the same mouse model reported reduced body weight on a chow diet (22). However, a TBC1D1$^{-/-}$ gene-trap mouse model, similar to the one used in our study, reported reduced body weight on both chow and the HFD (23). The discrepancy in the body weight phenotype is likely related to the mouse model used, the breeding strategy used to generate mice for experimental use (i.e., use of littermates vs. nonlittermates), the genetic background of the mice used, differences in the age of onset of the HFD, duration of the HFD, and specific composition (percentages and types of lipids) of the HFD. Genetic background clearly plays a crucial role in metabolism in mice (34), and it is now well recognized that breeding strategies and the degree of backcrossing affect the eventual metabolic phenotype. For this reason, all of our metabolic studies were performed using mice that were backcrossed onto a C57Bl/6 background for >10 generations, and all animals (TBC1D1$^{-/-}$ and WT) were littermates obtained from TBC1D1$^{+/-}$ breeding pairs.

We did, however, observe a significant reduction in GLUT4 levels in skeletal muscle from these mice (Fig. 2). This likely involves an important role for TBC1D1 in maintaining the stability of the GLUT4 protein, because we did not observe any change in GLUT4 mRNA, consistent with previous reports (22,24). The reduction in GLUT4 levels could be rescued by overexpression of TBC1D1 in TA muscle (Fig. 3). Notably, GLUT4 levels were significantly reduced only in muscle types that expressed little AS160 (Fig. 2). This indicates that in muscles expressing high levels of AS160, AS160

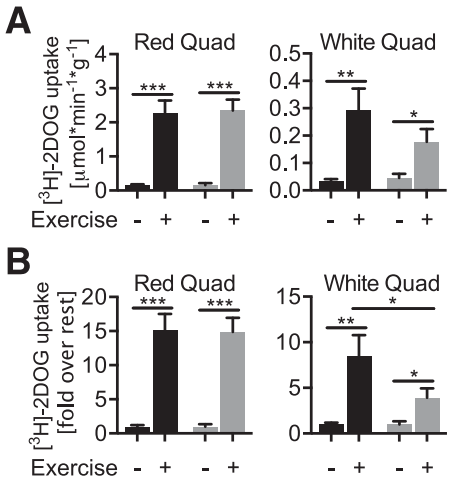

Figure 8—Exercise-mediated glucose uptake is impaired in white quadriceps from TBC1D1$^{-/-}$ mice. Resting or exercising mice (16.5 m/min treadmill running) were administered [^{3}H]-2DOG via intra-arterial injection. Mice were killed after 20 min, and red and white quadriceps (Quad) were collected. *A*: [^{3}H]-2DOG uptake is shown. *B*: [^{3}H]-2DOG uptake data in *A* are presented as fold over rest. WT is shown in black bars and KO in gray bars (n = 6–8). *P < 0.05, **P < 0.01, ***P < 0.001.

compensates for the loss of TBC1D1 in stabilizing GLUT4 levels in those muscles. Intriguingly, reduced GLUT4 levels have been observed in red muscle and fat from AS160$^{-/-}$ mice (43). This is consistent with a major role for these RabGAPs in regulating intracellular retention of GLUT4 in intracellular vesicles. In the absence of stimulation, TBC1D1 and AS160 are localized to GLUT4 vesicles via their interaction with IRAP. Under these circumstances, TBC1D1 and AS160 are nonphosphorylated, and their GAP activity is likely on, thus maintaining a Rab inactive. This leads to efficient intracellular sequestration of GLUT4. In the absence of TBC1D1 or AS160, GLUT4 vesicles are not efficiently sequestered, resulting in entry of GLUT4 into the endocytic recycling system and ultimately leading to increased delivery to the lysosome and GLUT4 degradation. Consistent with this, the half-life of the GLUT4 protein is ~50 h in the absence of insulin, and this is reduced to ~15 h in insulin-stimulated adipocytes (44). Hence, we conclude that in the absence of TBC1D1, GLUT4 protein levels are reduced in certain muscles that are normally enriched in TBC1D1 but not in AS160 expression, possibly due to increased GLUT4 degradation.

Another question arising from the current studies is why, in view of a 40% reduction in total GLUT4 levels in muscle, did we not observe any significant defect in whole-body insulin action? Previous studies using muscle-specific GLUT4$^{+/-}$ mice observed a concomitant impairment in glucose homeostasis and insulin action in muscle (45). However, GLUT4 levels in these studies were reduced in all muscles, including oxidative type muscles, whereas that was not the case in TBC1D1$^{-/-}$ mice. Given that red muscles are much more insulin sensitive than white muscles (46), this is consistent with a greater contribution of red muscle to whole-body insulin action. Importantly, insulin-stimulated glucose uptake was normal in isolated soleus from TBC1D1$^{-/-}$ mice (Fig. 7). Although there was an absolute reduction in insulin-stimulated [^{3}H]-2DOG uptake into EDL from TBC1D1$^{-/-}$ mice compared with WT mice, likely due to the 40% reduction in GLUT4 protein levels (Fig. 2), it is important to note that the fold increase over basal with insulin was almost identical in TBC1D1$^{-/-}$ EDL and in WT EDL (Fig. 7). Thus, it seems likely that the insulin-dependent increase in muscle glucose uptake, combined with the lesser contribution of white muscle to whole-body glucose metabolism, contributed to normal whole-body glucose and insulin tolerance in TBC1D1$^{-/-}$ mice (Fig. 4). This is consistent with other studies using different TBC1D1$^{-/-}$ mouse models that also showed no defect in glucose and insulin tolerance (22–24).

These studies provide further insights into the molecular regulation of glucose metabolism in muscle during exercise, implicating a key role for the RabGAP TBC1D1 in this process. We have not, however, been able to observe any significant role for this protein in obesity or whole-body insulin sensitivity.

Acknowledgments. The TBC1D1$^{-/-}$ mice were generated by the Australian Phenomics Network (APN) ES to Mouse service at Monash University. The authors thank Jørgen Jensen (Norwegian School of Sport Sciences, Oslo, Norway) for technical assistance with muscle isolation.

Funding. This work was supported by National Health and Medical Research Council (NHMRC) project grants GNT1068469 to J.S., GNT1047067 to D.E.J., and a grant from the Diabetes Australia Research Trust to J.S. D.E.J. is an NHMRC Senior Principal Research Fellow.

Duality of Interest. No potential conflicts of interest relevant to this article were reported.

Author Contributions. J.S. performed most of the experiments, designed the study, and wrote the manuscript. C.C.M., N.J.H., D.J.F., H.P., M.K., and G.J.C performed animal experiments. M.E.C. performed in vivo electroporation. X.M. performed quantitative PCR. A.E.B. performed the mouse surgery. J.A.L. initiated the study and organized the generation of the animal model. D.E.J. designed the study and wrote the manuscript. D.E.J. is the guarantor of this work and, as such, had full access to all the data in the study and takes responsibility for the integrity of the data and the accuracy of the data analysis.

References

1. Stöckli J, Fazakerley DJ, James DE. GLUT4 exocytosis. J Cell Sci 2011;124:4147–4159

2. Richter EA, Hargreaves M. Exercise, GLUT4, and skeletal muscle glucose uptake. Physiol Rev 2013;93:993–1017

3. Sano H, Kane S, Sano E, et al. Insulin-stimulated phosphorylation of a Rab GTPase-activating protein regulates GLUT4 translocation. J Biol Chem 2003;278:14599–14602

4. Hutagalung AH, Novick PJ. Role of Rab GTPases in membrane traffic and cell physiology. Physiol Rev 2011;91:119–149

5. Larance M, Ramm G, Stöckli J, et al. Characterization of the role of the Rab GTPase-activating protein AS160 in insulin-regulated GLUT4 trafficking. J Biol Chem 2005;280:37803–37813

6. Martin S, Rice JE, Gould GW, Keller SR, Slot JW, James DE. The glucose transporter GLUT4 and the aminopeptidase vp165 colocalise in tubulo-vesicular elements in adipocytes and cardiomyocytes. J Cell Sci 1997;110:2281–2291

7. Peck GR, Ye S, Pham V, et al. Interaction of the Akt substrate, AS160, with the glucose transporter 4 vesicle marker protein, insulin-regulated aminopeptidase. Mol Endocrinol 2006;20:2576–2583
8. Mîinea CP, Sano H, Kane S, et al. AS160, the Akt substrate regulating GLUT4 translocation, has a functional Rab GTPase-activating protein domain. Biochem J 2005;391:87–93
9. Sano H, Eguez L, Teruel MN, et al. Rab10, a target of the AS160 Rab GAP, is required for insulin-stimulated translocation of GLUT4 to the adipocyte plasma membrane. Cell Metab 2007;5:293–303
10. Ramm G, Larance M, Guilhaus M, James DE. A role for 14-3-3 in insulin-stimulated GLUT4 translocation through its interaction with the RabGAP AS160. J Biol Chem 2006;281:29174–29180
11. Eguez L, Lee A, Chavez JA, et al. Full intracellular retention of GLUT4 requires AS160 Rab GTPase activating protein. Cell Metab 2005;2:263–272
12. Brewer PD, Romenskaia I, Kanow MA, Mastick CC. Loss of AS160 Akt substrate causes Glut4 protein to accumulate in compartments that are primed for fusion in basal adipocytes. J Biol Chem 2011;286:26287–26297
13. Roach WG, Chavez JA, Mîinea CP, Lienhard GE. Substrate specificity and effect on GLUT4 translocation of the Rab GTPase-activating protein Tbc1d1. Biochem J 2007;403:353–358
14. Taylor EB, An D, Kramer HF, et al. Discovery of TBC1D1 as an insulin-, AICAR-, and contraction-stimulated signaling nexus in mouse skeletal muscle. J Biol Chem 2008;283:9787–9796
15. An D, Toyoda T, Taylor EB, et al. TBC1D1 regulates insulin- and contraction-induced glucose transport in mouse skeletal muscle. Diabetes 2010;59:1358–1365
16. Frøsig C, Pehmøller C, Birk JB, Richter EA, Wojtaszewski JF. Exercise-induced TBC1D1 Ser237 phosphorylation and 14-3-3 protein binding capacity in human skeletal muscle. J Physiol 2010;588:4539–4548
17. Jessen N, An D, Lihn AS, et al. Exercise increases TBC1D1 phosphorylation in human skeletal muscle. Am J Physiol Endocrinol Metab 2011;301:E164–E171
18. Tan SX, Ng Y, Burchfield JG, et al. The Rab GTPase-activating protein TBC1D4/AS160 contains an atypical phosphotyrosine-binding domain that interacts with plasma membrane phospholipids to facilitate GLUT4 trafficking in adipocytes. Mol Cell Biol 2012;32:4946–4959
19. Chen S, Murphy J, Toth R, Campbell DG, Morrice NA, Mackintosh C. Complementary regulation of TBC1D1 and AS160 by growth factors, insulin and AMPK activators. Biochem J 2008;409:449–459
20. Stone S, Abkevich V, Russell DL, et al. TBC1D1 is a candidate for a severe obesity gene and evidence for a gene/gene interaction in obesity predisposition. Hum Mol Genet 2006;15:2709–2720
21. Meyre D, Farge M, Lecoeur C, et al. R125W coding variant in TBC1D1 confers risk for familial obesity and contributes to linkage on chromosome 4p14 in the French population. Hum Mol Genet 2008;17:1798–1802
22. Chadt A, Immisch A, de Wendt C, et al. Deletion of both Rab-GTPase-activating proteins TBC1D1 and TBC1D4 in mice eliminates insulin- and AICAR-stimulated glucose transport [published correction appears in Diabetes 2015;64:1492]. Diabetes 2015;64:746–759
23. Dokas J, Chadt A, Nolden T, et al. Conventional knockout of Tbc1d1 in mice impairs insulin- and AICAR-stimulated glucose uptake in skeletal muscle. Endocrinology 2013;154:3502–3514
24. Szekeres F, Chadt A, Tom RZ, et al. The Rab-GTPase-activating protein TBC1D1 regulates skeletal muscle glucose metabolism. Am J Physiol Endocrinol Metab 2012;303:E524–E533
25. Chadt A, Leicht K, Deshmukh A, et al. Tbc1d1 mutation in lean mouse strain confers leanness and protects from diet-induced obesity. Nat Genet 2008;40:1354–1359
26. Hashiramoto M, James DE. Characterization of insulin-responsive GLUT4 storage vesicles isolated from 3T3-L1 adipocytes. Mol Cell Biol 2000;20:416–427
27. James DE, Strube M, Mueckler M. Molecular cloning and characterization of an insulin-regulatable glucose transporter. Nature 1989;338:83–87
28. Cleasby ME, Davey JR, Reinten TA, et al. Acute bidirectional manipulation of muscle glucose uptake by in vivo electrotransfer of constructs targeting glucose transporter genes. Diabetes 2005;54:2702–2711
29. Li J, Cantley J, Burchfield JG, et al. DOC2 isoforms play dual roles in insulin secretion and insulin-stimulated glucose uptake. Diabetologia 2014;57:2173–2182
30. James DE, Kraegen EW, Chisholm DJ. Muscle glucose metabolism in exercising rats: comparison with insulin stimulation. Am J Physiol 1985;248:E575–E580
31. Hoehn KL, Turner N, Swarbrick MM, et al. Acute or chronic upregulation of mitochondrial fatty acid oxidation has no net effect on whole-body energy expenditure or adiposity. Cell Metab 2010;11:70–76
32. Prabhu AV, Krycer JR, Brown AJ. Overexpression of a key regulator of lipid homeostasis, Scap, promotes respiration in prostate cancer cells. FEBS Lett 2013;587:983–988
33. Arola L, Herrera E, Alemany M. A new method for deproteinization of small samples of blood plasma for amino acid determination. Anal Biochem 1977;82:236–239
34. Montgomery MK, Hallahan NL, Brown SH, et al. Mouse strain-dependent variation in obesity and glucose homeostasis in response to high-fat feeding. Diabetologia 2013;56:1129–1139
35. Cartee GD, Funai K. Exercise and insulin: convergence or divergence at AS160 and TBC1D1? Exerc Sport Sci Rev 2009;37:188–195
36. Dash S, Sano H, Rochford JJ, et al. A truncation mutation in TBC1D4 in a family with acanthosis nigricans and postprandial hyperinsulinemia. Proc Natl Acad Sci U S A 2009;106:9350–9355
37. Dash S, Langenberg C, Fawcett KA, et al. Analysis of TBC1D4 in patients with severe insulin resistance. Diabetologia 2010;53:1239–1242
38. Furler SM, Goldstein M, Cooney GJ, Kraegen EW. In vivo quantification of glucose uptake and conversion to glycogen in individual muscles of the rat following exercise. Metabolism 1998;47:409–414
39. Pehmøller C, Treebak JT, Birk JB, et al. Genetic disruption of AMPK signaling abolishes both contraction- and insulin-stimulated TBC1D1 phosphorylation and 14-3-3 binding in mouse skeletal muscle. Am J Physiol Endocrinol Metab 2009;297:E665–E675
40. Maarbjerg SJ, Jørgensen SB, Rose AJ, et al. Genetic impairment of AMPKalpha2 signaling does not reduce muscle glucose uptake during treadmill exercise in mice. Am J Physiol Endocrinol Metab 2009;297:E924–E934
41. Merry TL, Steinberg GR, Lynch GS, McConell GK. Skeletal muscle glucose uptake during contraction is regulated by nitric oxide and ROS independently of AMPK. Am J Physiol Endocrinol Metab 2010;298:E577–E585
42. O'Neill HM, Maarbjerg SJ, Crane JD, et al. AMP-activated protein kinase (AMPK) beta1beta2 muscle null mice reveal an essential role for AMPK in maintaining mitochondrial content and glucose uptake during exercise. Proc Natl Acad Sci U S A 2011;108:16092–16097
43. Lansey MN, Walker NN, Hargett SR, Stevens JR, Keller SR. Deletion of Rab GAP AS160 modifies glucose uptake and GLUT4 translocation in primary skeletal muscles and adipocytes and impairs glucose homeostasis. Am J Physiol Endocrinol Metab 2012;303:E1273–E1286
44. Sargeant RJ, Pâquet MR. Effect of insulin on the rates of synthesis and degradation of GLUT1 and GLUT4 glucose transporters in 3T3-L1 adipocytes. Biochem J 1993;290:913–919
45. Zisman A, Peroni OD, Abel ED, et al. Targeted disruption of the glucose transporter 4 selectively in muscle causes insulin resistance and glucose intolerance. Nat Med 2000;6:924–928
46. James DE, Jenkins AB, Kraegen EW. Heterogeneity of insulin action in individual muscles in vivo: euglycemic clamp studies in rats. Am J Physiol 1985;248:E567–E574